Original Research Article

Active and Time delay Controls on Dynamical of The Micro-Electro-Mechanical System (MEMS) Resonator

Abstract

In this paper, the active control and time delay control are applied on a nonlinear dynamic mechanical system subjected to external force to reduce the resulted vibration. The system is modeled by a unique nonlinear differential equation. We applied the technique of multiple scale perturbation to obtain an approximate solution and showing the response equation. The primary resonance case is investigated to study the stability and the steady-state response of the system. Also we studied the linearity of the solution. MATLAB 14.0 and Maple 18.0 programs were used to study the numerical solution and the effect of the different parameters for the response of the nonlinear dynamic mechanical system.

Keywords

Nonlinear dynamical system, Active Control, time delay, multiple scale perturbation method.

1. Introduction

In recent years, several investigations have reported how to control the vibration of dynamical systems. The dynamic absorber is one of the most common methods of vibration control that it has low cost, simple operation and taking advantage of the saturation phenomenon. This phenomenon has been observed in the forced vibrations of coupled two degrees of freedom systems with quadratic nonlinearities in the presence of both internal and primary resonances. Vazquez-Gonzalez and Silva Navarro [1] discussed the dynamic response and nonlinear frequency analysis of a damped Duffing system attached to an autoparametric pendulum absorber, operating under the external and internal resonance conditions. They deduced that is possible to reduce simultaneously the amplitude responses of the primary and secondary systems for excitation frequencies close to the exact tuning.

Eissa et al. [2] reported the results of studying the vibration reduction of a nonlinear spring pendulum subjected to multi external and parametric excitations. They investigated that the vibration of a ship pitch-roll motion can be reduced using a longitudinal absorber. Active absorber for non-linear vibrating system subjected to external and parametric forces is investigated by Sayed and Kamel [3]. Sado [4] described the numerical simulation of a nonlinear two-mass auto parametric system with elastic pendulum hangs down from the flexible suspended body. He showed that near the internal and external resonances depending on a selection of physical system parameters, the amplitudes of vibrations of coupled modes may be differently.

Wenzhi and Zhiyong [5] studied active control of torsional vibration of a large turbo-generator. They found that full state feedback control with linear quadratic regulator (LQR) has significant e□ectiveness on attenuation of torsional vibration energy and response of the turbo-generator's shaft system.

UNDER PEER REVIEW

Amer et al. [6] used two active control laws based on the linear negative velocity and acceleration feedback and showed that the acceleration feedback was good for the main system. Hegazy and Salem [7] presented the numerical and perturbation solutions of an inclined beam to external and parametric forces with two different controllers, positive position feedback (PPF) and nonlinear saturation controllers (NSC) and found that the (NSC) one is an effective controller.

El-Gohary and El-Ganaini [8] studied applying a time delay absorber to suppress chaotic vibrations of a beam under multi-parametric excitations. They concluded that the vibration of the main system can be reduced. They showed that time-delay effect on the frequency response curves is trivial. Maccari [9] investigated the periodic solutions for parametrically excited system under state feedback control with a time delay. He has derived two slow-flow equations, governing the amplitude and phase of approximate long time response. Elnaggar and Khalil [10] investigated the response of nonlinear system subjected to external excitation controlled by the appropriate choice of feedback gains and two distinct time delays. They found that a suitable choice of the feedback gains and time-delays can enlarge the critical force amplitude, and reduce the peak amplitude of the response (or peak amplitude of the free oscillation term) for the case of primary resonance or for the case of super harmonic resonance. El-Bassiouny and El-Kholy [11] discussed the resonances of a nonlinear single-degree-of-freedom system with time delay in linear feedback control. They observed from the frequency-response curves of primary resonance that the response amplitude loses stability for increasing time delay.

A study for (NSC) is presented by Hamed and Amer [12] that used to suppress the vibration amplitude of a structural dynamic model simulating nonlinear composite beam at simultaneous sub-harmonic and internal resonance excitation. Kamel et al. [13] studied the active vibration control of a nonlinear magnetic levitation system via (NSC). Warminski et al. [14] presented an application of (NSC) algorithm for a self-excited strongly nonlinear beam structure driven by an external force. The results show that the increase in controller damping may cancel the undesirable instability. Amer [15] investigated the behavior of the coupling of two non-linear oscillators of the system and absorber representing ultrasonic cutting process subjected to parametric excitation. He showed that the steady state amplitude of the main system is a monotonic increasing function of the excitation force amplitude up to a saturation value. The multiple scales method was used by Ebrahimi et al [16] to perform a nonlinear vibrational analysis of a sliding pendulum in two cases with dry and lubricated clearance joint. They investigated that in the primary resonance analysis, increasing the dynamic lubricant viscosity decreases the amplitude in the vicinity of the linear natural frequency as expected.

Amer and Abd Elsalam [17] studied the stability of a nonlinear two-degree of freedom system subjected to multi excitation forces at simultaneous primary and internal resonance case. They deduced that the steady state amplitude is monotonic increasing function of the excitation force amplitude increased and is a monotonic decreasing of the damping coefficient. The study of forced nonlinear vibrations of a simply supported Euler-Bernoulli beam resting on a nonlinear elastic foundation with quadratic and cubic nonlinearities with the homotopy analysis method has presented by Shahlaei-Far et al. [18]. The derived closed-form solution of the amplitude yields frequency response curves for various values of the quadratic and cubic nonlinearity coefficients presenting their softening/hardening-type effect on the distributed-parameter system.

Many applications of controlling the dynamical systems which investigated in more papers. Wang et al. [19] investigated the dynamic response and bifurcation characteristics of blades with varying rotating speed. The results of the paper showed the interaction of the fluid and the

UNDER PEER REVIEW

structure that the opposite varying trends for the amplitudes and phase angles with respect to the system parameters indicate the energy transfer between the vibrations of the fluid and the structure. Hamed et al. [20] were investigated the nonlinear vibrations and stability of the MEMS gyroscope subjected to different types of parametric excitations. They applied an active vibration controller to reduce the resulted vibration. A multi-modal flexible wind turbine model with variable rotor speed has been formulated by Staino and Basu [21] using a Lagrangian approach. They analyzed the e□ect of the rotational speed on the edgewise vibration of the blades. They deduced according to the numerical results which have been presented in their paper, a considerable deterioration of the structural response of the blade could occur caused by variations in the rotational speed due to an electrical fault.

Shao et al. [22] studied the effect of time-delayed feedback controller on the dynamics of electrostatic MEMS resonators. They compared the results of the perturbation method to the shooting technique and the basin-of-attraction analysis. They found that the shooting technique performs well in predicting the global stability for the resonator under negative gain control. In a MEMS system, Daqaq et al. [23] again used the method of multiple of scales to define a first-order nonlinear approximate solution, which was then employed to redefine the impulse sequence of a ZV input shaper to minimize residual oscillation in a torsional micromirror. Static and Dynamic Mechanical Behaviors of Electrostatic MEMS Resonator with Surface Processing Error is studied by Feng et al [24]. They showed the resonance frequency and bifurcation behavior through dynamic analysis.

In this work, we have studied the reducing of the vibration system that is described in [24] through dynamic analysis by applying both of active control and time delay control. The effect of the varying parameters of the system and comparing between the two controllers have reported.

2. Equation of Motion

Feng et al [24] have been studied a model considering the effect of surface machining error on the thickness of the microbeam. The thickness of the microbeam is not constant due to the processing errors. The schematic diagram of microbeam is shown in Fig. (1). The shape of the microbeam is controlled by adjusting the value of section parameter λ. (a) case of $\lambda > 0$ (b) case of $\lambda < 0$.

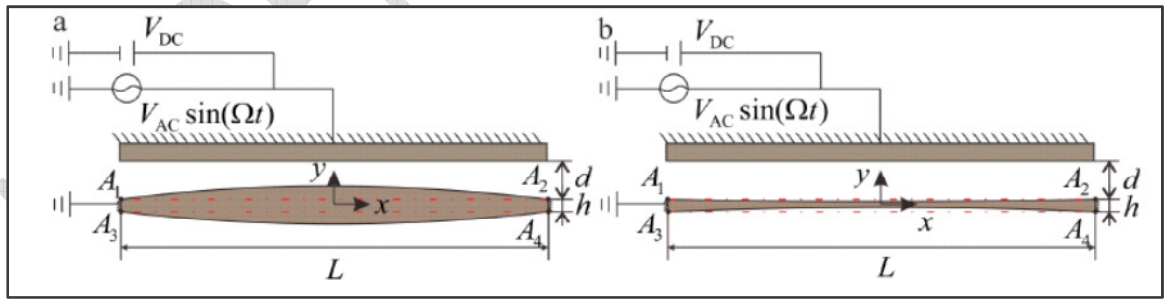

Fig. (1): The schematic diagram of microbeam.

The bending vibration equation of the system is obtained through force analysis. Since the main objective of [24] was to explore the main resonance problem in the nonlinear dynamics problem, the first-order mode is considered that it was sufficient to obtain good results. So, Galerkin method is applied to derive a reduced-order model, they expressed the deflection $y(x,t)$

UNDER PEER REVIEW

as: $y(x,t)=u(t)\phi(x)$, where $u(t)$ is the modal coordinate amplitude and $\phi(x)$ is the mode shapes of the normalized undamped linear orthonormal.

The resonance frequency and bifurcation behavior can be obtained through dynamic analysis. Feng et al [24] introduced the modal coordinate amplitude through dynamic analysis using the MMS to investigate the response of the microresonator with small vibration amplitude around the stable equilibrium positions as $u=u_s+u_A$, where

u_s is the response to DC voltage and u_A is the response to AC voltage. The terms representing the equilibrium position can be eliminated in the equation of motion that governs the transverse deflection. Since V_{AC} is far less than V_{DC} in the microresonator, the terms $V_{DC}=O(1)$, $V_{AC}=O(\varepsilon^3)$ and ε is regarded as a small non-dimensional parameter. So, Feng et al [24] modified the equation of the system as follows:

$$\ddot{u}_A+\omega_n{}^2u_A+\varepsilon^2\mu\dot{u}_A+a_qu_A{}^2+a_cu_A{}^3=\varepsilon^3f\cos(\omega t) \tag{1}$$

where:

u_A is the modal coordinate amplitude which to AC voltage, ω_n is the internal frequency, μ is the damping coefficient of the system, ω is the alternating current excitation frequency, f is the external excitation force, a_c and a_q are the nonlinear parameters.

3.1. Active Control

Using a negative linear velocity feedback controller connected to the nonlinear dynamical system; eqn. (1) can be represented as follows:

$$\ddot{u}+\omega^2u+\varepsilon^2\mu\dot{u}+a_qu^2+a_cu^3=\varepsilon^3f\cos(\Omega t)-\varepsilon^2G\dot{u} \tag{2}$$

We use the method of multiple scale

$$u(t,\varepsilon)=\varepsilon u_1(T_0,T_1,T_2)+\varepsilon^2u_2(T_0,T_1,T_2)+\varepsilon^3u_3(T_0,T_1,T_2) \tag{3}$$

where $T_k=\varepsilon^kt$. So, we can write that:

$$\frac{d}{dt}=D_0+\varepsilon D_1+\varepsilon^2D_2+\ldots,\ \frac{d^2}{dt^2}=D_0{}^2+\varepsilon(2D_0D_1)+\varepsilon^2\left(D_1{}^2+2D_0D_2\right)+\ldots \tag{4}$$

where $D_k=\dfrac{\partial}{\partial T_k}$, $(k=0,1,2)$.

Substituting equations (3) and (4) into equations (2), then equating the like order of ε, we get the following:

Order ε^1:

$$\left(D_0{}^2+\omega^2\right)u_1=0 \tag{5}$$

Order ε^2:

$$\left(D_0{}^2+\omega^2\right)u_2=-2D_0D_1u_1-a_qu_1{}^2 \tag{6}$$

Order ε^3:

$$\left(D_0{}^2+\omega^2\right)u_3=-2D_0D_1u_2-\left(D_1{}^2+2D_0D_2+\mu D_0\right)u_1-2a_qu_1u_2-a_cu_1{}^3+f\cos(\Omega t)-GD_0u_1 \tag{7}$$

The general solution of equation (5) can be expressed in the form:

$$u_1=A(T_1,T_2)e^{i\omega T_0}+\overline{A}(T_1,T_2)e^{-i\omega T_0} \tag{8}$$

Substituting equation (8) into equation (6), we can obtain the following:

UNDER PEER REVIEW

$$\left(D_0{}^2+\omega^2\right)u_2=-2i\omega\left[\left(\frac{\partial A}{\partial T_1}\right)e^{i\omega T_0}-\left(\frac{\partial \bar{A}}{\partial T_1}\right)e^{-i\omega T_0}\right]-a_q\left[A^2e^{2i\omega T_0}+2A\bar{A}+\bar{A}^2e^{-2i\omega T_0}\right] \quad (9)$$

The secular term is eliminated if:

$$-2i\omega\left(\frac{\partial A}{\partial T_1}\right)+cc.=0 \quad \rightarrow \quad \left(\frac{\partial A}{\partial T_1}\right)=0 \quad (10)$$

which indicates that A is only a function of T_2.

We get one resonance case as the primary resonance case: $\Omega\cong\omega$

So, we can represent the detuning parameter σ as follows:

$$\Omega=\omega+\varepsilon^2\sigma \quad (11)$$

So, the general solution of eqns. (6) and (7) can be written as:

$$u_2=\frac{a_q}{3\omega^2}A^2e^{2i\omega T_0}-\frac{2a_q}{\omega^2}A\bar{A}+\frac{a_q}{3\omega^2}\bar{A}^2e^{-2i\omega T_0} \quad (12)$$

$$u_3=\left(\frac{a_c}{8\omega^2}+\frac{1a_q{}^2}{12\mathrm{A}\omega^4}\right)A^3e^{3i\omega T_0}+cc. \quad (13)$$

By eliminating the secular term in eqn. (7), we get that:

$$-2i\omega\left(D_2A\right)-i\omega\mu A-3a_cA^2\bar{A}+\frac{10a_q{}^2}{3\omega^2}A^2\bar{A}-i\omega GA+\frac{f}{2}e^{i\sigma T_2}=0 \quad (14)$$

It is convenient to express A in the polar form:

$$A=\frac{1}{2}a\left(T_2\right)e^{i\beta(T_2)} \quad (15)$$

By substituting eqn. (15) into eqn. (14); separating the imaginary and real parts yield:

$$\dot{a}=-\left(\frac{\mu+G}{2}\right)a+\frac{f}{2\omega}\sin\theta \quad (16)$$

$$a\left(\sigma-\dot{\theta}\right)=\left(\frac{3a_c}{8\omega}-\frac{5a_q{}^2}{12\omega^3}\right)a^3-\frac{f}{2\omega}\cos\theta \quad (17)$$

Where, $\theta=\sigma T_2-\beta$ (18)

The steady-state response can be obtained by imposing the conditions: $\dot{a}=\dot{\theta}=0$

By applying the previous conditions, the frequency response equation can be derived as follows:

$$\sigma^2-\left(\frac{3a_c}{4\omega}-\frac{5a_q{}^2}{6\omega^3}\right)a^2\sigma+\left(\frac{3a_c}{8\omega}-\frac{5a_q{}^2}{12\omega^3}\right)^2a^4+\left(\frac{G+\mu}{2}\right)^2-\left(\frac{f}{2\omega a}\right)^2=0 \quad (19)$$

3.1.1. Linear Solution

To study the stability of the linear solution of the obtained fixed points, let us consider A, in the form:

$$A\left(T_2\right)=\frac{1}{2}\left(p-iq\right)e^{i\gamma T_2} \quad (20)$$

By substituting from eqn. (20) into the linear parts of eqn. (14) and equating real and imaginary parts; we get:

UNDER PEER REVIEW

$$\dot{p} = -\left(\frac{\mu+G}{2}\right)p - \gamma q$$

(21)

$$\dot{q} = \gamma p - \left(\frac{\mu+G}{2}\right)q \tag{22}$$

The Characteristic equation can be written as:

$$\left[\lambda + \left(\frac{\mu+G}{2}\right)\right]^2 + \gamma^2 = 0 \tag{23}$$

Easily we can deduce the solutions of the eqn. (23) as following:

$$\lambda_{1,2} = -\left(\frac{\mu+G}{2}\right) \pm i\gamma \tag{24}$$

So, the linear solution is stable everywhere that the real part is always negative.

3.1.2 Nonlinear solution:

To study the stability of the nonlinear solution of the obtained fixed points, let:

$$a = a_0 + a_1,\ \theta = \theta_0 + \theta_1 \tag{25}$$

where a_0, θ_0 are the solutions of eqns. (16) and (17) and a_1, θ_1 are perturbations which are assumed to be small compared with a_0, θ_0.

Substituting equation (25) into equations (16) and (17) and keeping only the linear terms in a_1, θ_1, gives:

$$\dot{a}_1 = -\left(\frac{\mu+G}{2}\right)a_1 + \frac{f}{2\omega}\cos(\theta_0)\theta_1 \tag{26}$$

$$\dot{\theta}_1 = \left(\frac{\sigma}{a_0} - \left(\frac{9a_c}{8\omega} - \frac{5a_q{}^2}{4\omega^3}\right)a_0\right)a_1 - \frac{f}{2\omega a_0}\sin(\theta_0)\theta_1 \tag{27}$$

We can express the characteristic equation as:

$$\lambda^2 + \left(\frac{f}{2\omega a_0}\sin(\theta_0) + \left(\frac{\mu+G}{2}\right)\right)\lambda - \left(\frac{\sigma}{a_0} - \left(\frac{9a_c}{8\omega} - \frac{5a_q{}^2}{4\omega^3}\right)a_0\right)\frac{f}{2\omega}\cos(\theta_0)$$

$$+\left(\frac{\mu+G}{2}\right)\frac{f}{2\omega a_0}\sin(\theta_0) = 0 \tag{28}$$

So, the solutions of eqn. (29) are:

$$\lambda_{1,2} = -\frac{1}{4}\left(\mu + G + \frac{f}{\omega a_0}\sin(\theta_0)\right) \pm \frac{1}{4}\sqrt{\left(\mu + G + \frac{f}{\omega a_0}\sin(\theta_0)\right)^2 - 16\mathrm{K}} \tag{29}$$

$$\text{where } \mathrm{K} = \left(\frac{\mu+G}{2}\right)\frac{f}{2\omega a_0}\sin(\theta_0) - \left(\frac{\sigma}{a_0} - \left(\frac{9a_c}{8\omega} - \frac{5a_q{}^2}{4\omega^3}\right)a_0\right)\frac{f}{2\omega}\cos(\theta_0) \tag{30}$$

If the real part of the eigenvalue is negative, then the linear solution is stable; otherwise, it is unstable.

UNDER PEER REVIEW

3.1.3. Numerical Solution

The Runge-Kutta fourth-order method has been applied to determine the numerical solution of the equation (2) as shown in Figure 2 at the selected values: $(\Omega = 3.066,\ \omega = 3.066,\ \mu = 0.003,$ $a_q = 1, a_c = 1, f = 1.8, G = 4)$. Figure 2 shows the effect of using active control on the amplitude of the main system. Numerical solution of the response equation represented in equation (19) have been discussed. Figure 3 illustrates the effect of the varying parameters on the response curve at the primary resonance case $\Omega \cong \omega$ under effect of the gain feedback controller. The solid line represents the stable region. While, the dotted line represents the unstable region. Figure (3a) shows that the parameter of the natural frequency has hardening and softening nonlinearity effect. The effect of the damping coefficient on the response curve is illustrated in Figure (3b). It shows that the amplitude is monotonic decreasing function and the amplitude is bent to right. The effect of nonlinear parameters is shown in Figures (3c) and (3d). Figure (3c) shows that the amplitude is monotonic decreasing function in the nonlinear parameter a_c and the amplitude is bent to right. Figure (3d) shows that the nonlinear parameter a_q has hardening and softening nonlinearity effect. The amplitude is monotonic increasing with varying of the excitation force f and the amplitude is bent to right. It is shown in Figure (3e). Figure (3f) illustrates that the amplitude is monotonic decreasing function in the parameter of gain feedback controller G.

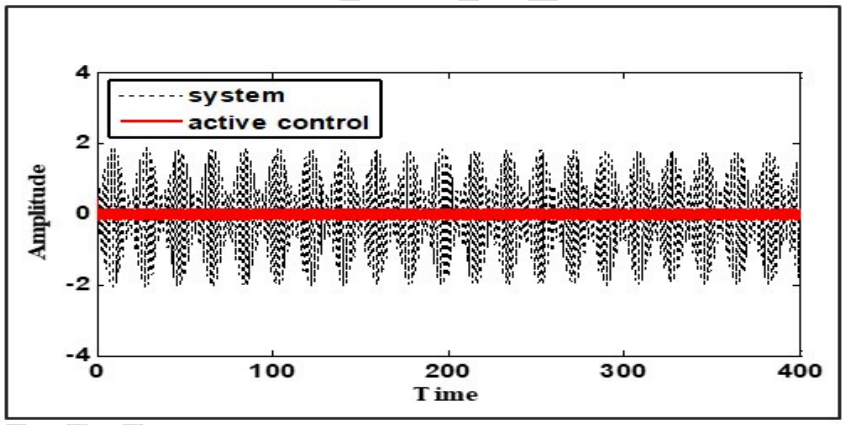

Fig. (2): The time history of the main system and active control at primary resonance case $\Omega \cong \omega$

UNDER REVIEW

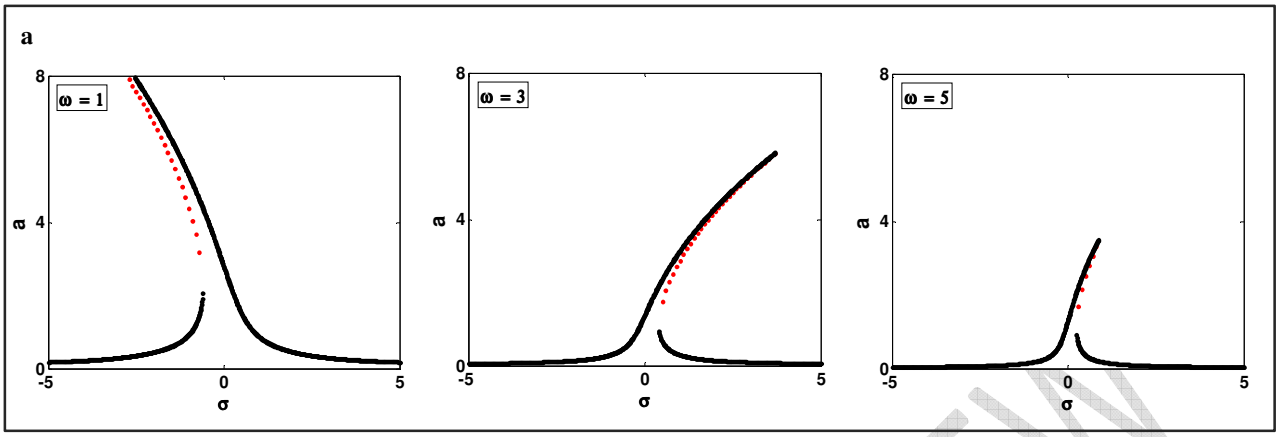

Fig. (3a): effect of ω, the values of the parameters are: $\mu = 0.003, a_q = 1, a_c = 1, f = 1.8, G = 0.1$.

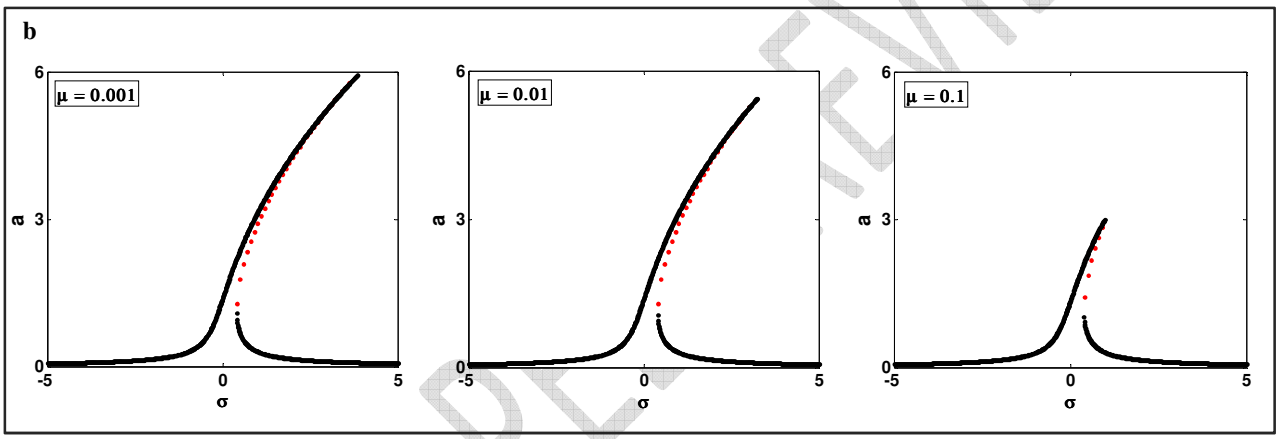

Fig. (3b): effect of μ, the values of the parameters are: $\omega = 3.066, a_q = 1, a_c = 1, f = 1.8, G = 0.1$.

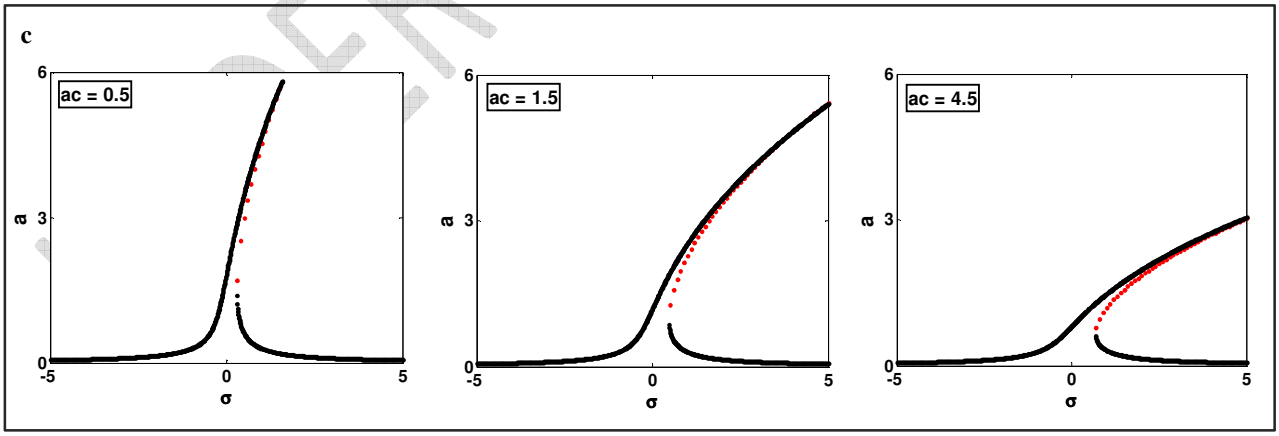

Fig. (3c): effect of a_c, the values of the parameters are: $\omega = 3.066, \mu = 0.003, a_q = 1, f = 1.8, G = 0.1$.

UNDER PEER REVIEW

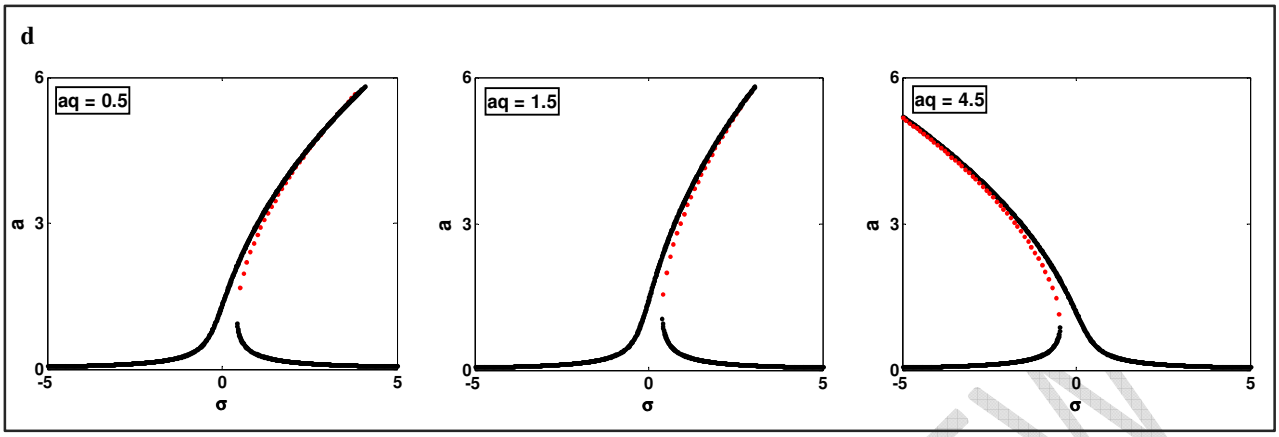

Fig. (3d): effect of a_q , the values of the parameters are:

$\omega = 3.066, \mu = 0.003, a_c = 1, f = 1.8, G = 0.1$.

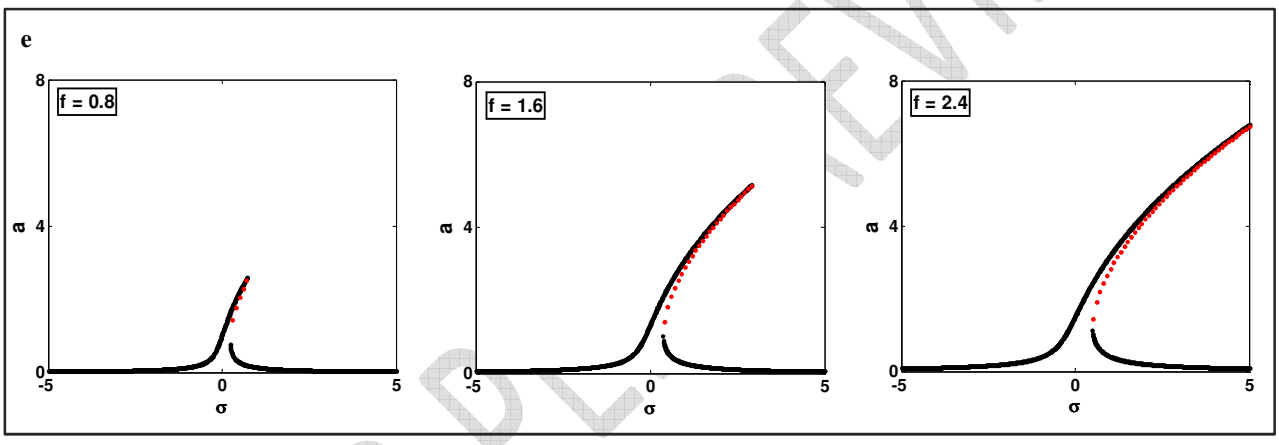

Fig. (3e): effect of f , the values of the parameters are:

$\omega = 3.066, \mu = 0.003, a_c = 1, a_q = 1, G = 0.1$.

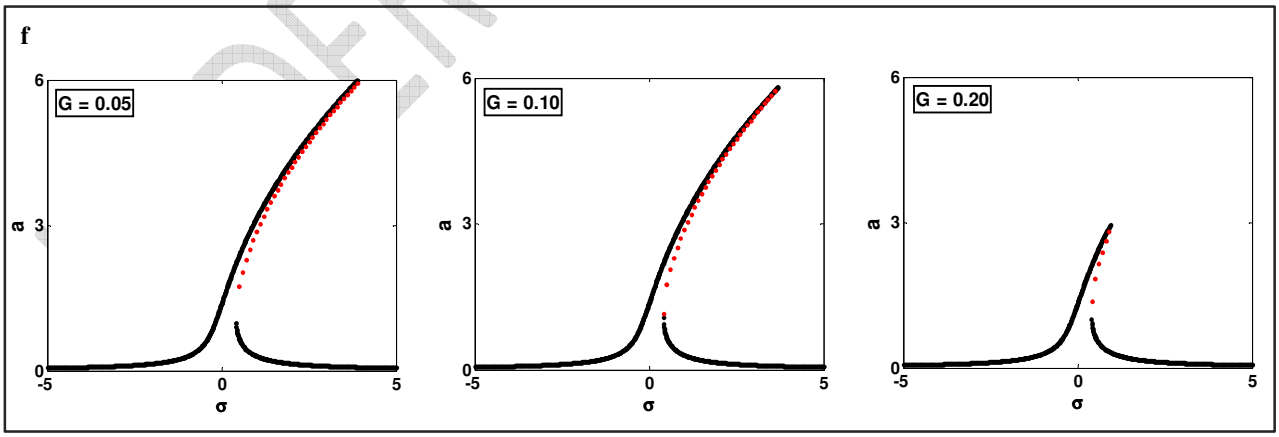

Fig. (3f): effect of G , the values of the parameters are:

$\omega = 3.066, \mu = 0.003, a_c = 1, a_q = 1, f = 1.8$.

PREPRINT REVIEW

3.1.4. Comparison between the perturbation and the numerical solution

The comparison of the analytical solution - given by equations (26) and (27) - and the approximate solution of equation (2) at the case of active control have been shown in Figure (4) and Figure (5). Figure (4) described the comparison in the time history and Figure (5) described the comparison in the response curve. Figures (4) and (5) show that there is a good agreement between both analytical and numerical solutions.

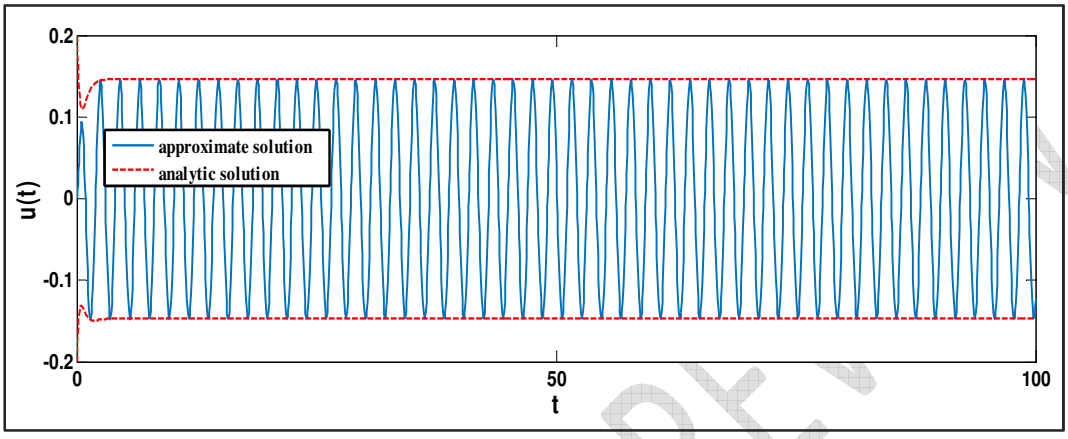

Fig. (4): Comparison between the analytic solution and the approximate solution at the case of active control (Time history).

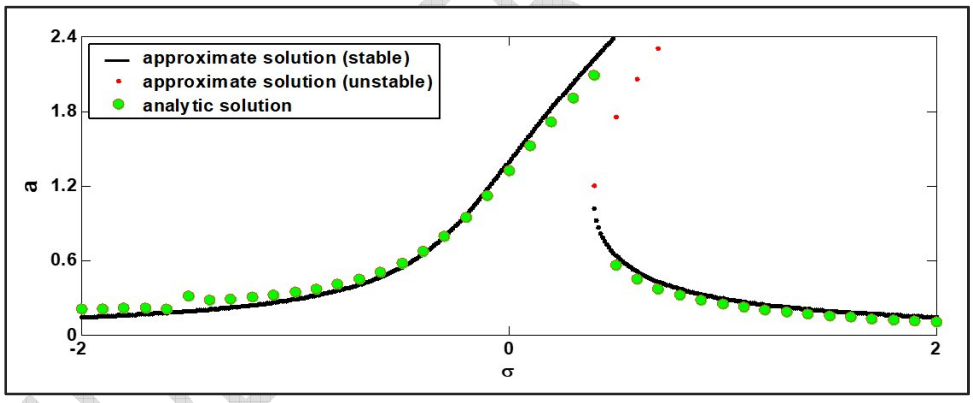

Fig. (5): Comparison between the analytic solution and the approximate solution at the case of active control (Response curve).

3.2.Time delay Control:

The equation of system under consideration using time delay control is represented as follows:

$$\ddot{u}(t)+\omega^2 u(t)+\varepsilon^2\mu\dot{u}(t)+a_q u^2(t)+a_c u^3(t)=\varepsilon^3 f\cos(\Omega t)-\varepsilon^2 G\dot{u}(t-\tau) \quad (31)$$

The secular term will be:

$$-2i\omega(D_2 A)-i\omega\mu A-3a_c A^2\bar{A}+\frac{10a_q^{\,2}}{3\omega^2}A^2\bar{A}-i\omega GAe^{-i\omega\tau}+\frac{f}{2}e^{i\sigma T_2}=0 \quad (32)$$

By substituting eqn. (15) into eqn. (32); separating the imaginary and real parts yield:

$$\dot{a} = -\frac{\mu}{2}a - \frac{G}{2}a\cos(\omega\tau) + \frac{f}{2\omega}\sin\theta \tag{33}$$

$$a(\sigma - \dot{\theta}) = \frac{G}{2}a\sin(\omega\tau) + \left(\frac{3a_c}{8\omega} - \frac{5a_q{}^2}{12\omega^3}\right)a^3 - \frac{f}{2\omega}\cos\theta \tag{34}$$

Finally, by applying the conditions $\dot{a} = \dot{\theta} = 0$; the frequency response equation can be derived as follows:

$$\sigma^2 - \left[\left(\frac{3a_c}{4\omega} - \frac{5a_q{}^2}{6\omega^3}\right)a^2 + G\sin(\omega\tau)\right]\sigma + \left(\frac{3a_c}{8\omega} - \frac{5a_q{}^2}{12\omega^3}\right)^2 a^4 + \left(\frac{3a_c}{8\omega} - \frac{5a_q{}^2}{12\omega^3}\right)Ga^2\sin(\omega\tau) + \frac{\mu G}{2}\cos(\omega\tau)$$

$$+\frac{\mu^2 + G^2}{4} - \left(\frac{f}{2\omega a}\right)^2 = 0 \tag{35}$$

3.2.1. Linear Solution

Put: $A(T_2) = \frac{1}{2}(p - iq)e^{i\gamma T_2}$ into the linear parts of eqn. (32) to study the stability of the linear solution; we get after equating real and imaginary parts:

$$\dot{p} = -\left(\frac{\mu}{2} + \frac{G}{2}\cos(\omega\tau)\right)p - \left(\gamma - \frac{G}{2}\sin(\omega\tau)\right)q \tag{36}$$

$$\dot{q} = \left(\gamma - \frac{G}{2}\sin(\omega\tau)\right)p - \left(\frac{\mu}{2} + \frac{G}{2}\cos(\omega\tau)\right)q \tag{37}$$

The Characteristic Eqn. can be expressed as follows:

$$4\lambda^2 + 4\left(\mu + G\cos(\omega\tau)\right)\lambda + \left(\mu^2 + G^2 + 4\gamma^2 + 2\mu G\cos(\omega\tau) - 4\gamma G\sin(\omega\tau)\right) = 0 \tag{38}$$

The solutions of eqn. (38) are:

$$\lambda_{1,2} = \frac{1}{2}\left(\mu + G\cos(\omega\tau)\right) \pm \frac{1}{2}\sqrt{\left(\mu + G\cos(\omega\tau)\right)^2 - \left(\mu^2 + G^2 + 4\gamma^2 + 2\mu G\cos(\omega\tau) - 4\gamma G\sin(\omega\tau)\right)} \tag{39}$$

So; the linear solution is stable only if the real part of the eigenvalue in eqn. (39) is negative.

3.2.2. Nonlinear Solution

Putting: $a = a_0 + a_1$, $\theta = \theta_0 + \theta_1$ into eqns. (33) and (34); we can deduce that:

$$\dot{a}_1 = -\left(\frac{\mu}{2} + \frac{G}{2}\cos(\omega\tau)\right)a_1 + \frac{f}{2\omega}\cos(\theta_0)\theta_1 \tag{40}$$

$$\dot{\theta}_1 = \left(\frac{\sigma}{a_0} - \frac{G}{2a_0}\sin(\omega\tau) - \left(\frac{9a_c}{8\omega} - \frac{5a_q{}^2}{4\omega^3}\right)a_0\right)a_1 - \frac{f}{2\omega a_0}\sin(\theta_0)\theta_1 \tag{41}$$

We can write the characteristic equation and its solutions as follows:

$$\lambda^2 + \frac{1}{2}\left(\mu + G\cos(\omega\tau) + \frac{f}{\omega a_0}\sin(\theta_0)\right)\lambda + \mathrm{H} = 0$$

(42)

where $\mathrm{H} = \left(\frac{\mu}{2} + \frac{G}{2}\cos(\omega\tau)\right)\frac{f}{2\omega a_0}\sin(\theta_0) - \left(\frac{\sigma}{a_0} - \frac{G}{2a_0}\sin(\omega\tau) - \left(\frac{9a_c}{8\omega} - \frac{5a_q{}^2}{4\omega^3}\right)a_0\right)\frac{f}{2\omega}\cos(\theta_0)$

UNDER PEER REVIEW

$$\lambda_{1,2}=\frac{1}{4}\left(\mu+G\cos(\omega\tau)+\frac{f}{\omega a_0}\sin(\theta_0)\right)\pm\frac{1}{8}\sqrt{\left(\mu+G\cos(\omega\tau)+\frac{f}{\omega a_0}\sin(\theta_0)\right)^2+64\mathrm{H}} \quad (43)$$

If the real part of the eigenvalue is negative, then the linear solution is stable; otherwise, it is unstable.

3.2.3. Numerical Solution:

The Runge-Kutta fourth-order method has been applied to determine the numerical solution of the equation (31) as shown in Figure 6 at the selected values: $(\Omega=3.066,\ \omega=3.066,\ \mu=0.003,$ $a_q=1, a_c=1, f=1.8, G=4, \tau=0.1)$. Figure 6 shows the effect of using time delay control on the amplitude of the main system. Numerical solution of the response equation represented in equation (35) have been discussed. Figure 7 illustrates the effect of the varying parameters on the response curve at the primary resonance case $\Omega\cong\omega$ under effect of the time delay controller. The solid line represents the stable region. While, the dotted line represents the unstable region. Figure (7a) shows that the parameter of the natural frequency has hardening and softening nonlinearity effect. The effect of the damping coefficient on the response curve is illustrated in Figure (7b). It shows that the amplitude is monotonic decreasing function and the amplitude is bent to right. The effect of nonlinear parameters is shown in Figures (7c) and (7d). Figure (7c) shows that the amplitude is monotonic decreasing function in the nonlinear parameter a_c and the amplitude is bent to right. Figure (7d) shows that the nonlinear parameter a_q has hardening and softening nonlinearity effect. The amplitude is monotonic increasing with varying of the excitation force f and the amplitude is bent to right. It is shown in Figure (7e). Figure (7f) illustrates that the amplitude is monotonic decreasing function in the parameter of gain feedback controller G. Fig. (7g) shows that the amplitude is monotonic increasing function in the parameter of time delay controller τ.

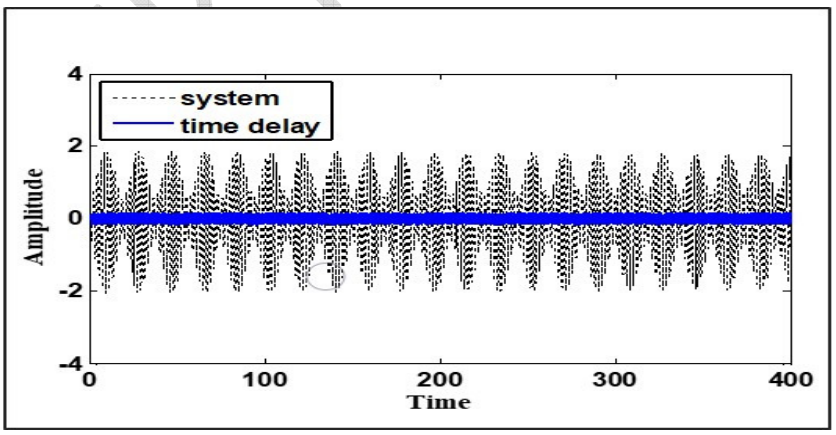

Fig. (6): The time history of the main system and time delay control at primary resonance case $\Omega\cong\omega$

3.2.4. Comparison between the perturbation and the numerical solution

The comparison of the analytical solution - given by equations (40), (41) and the approximate solution of equation (31) at the case of time delay control have been shown in Figure (8) and Figure (9). Figure (8) described the comparison in the time history and Figure (9)

UNDER PEER REVIEW

described the comparison in the response curve. Figures (8) and (9) show that there is a good agreement between both analytical and numerical solutions.

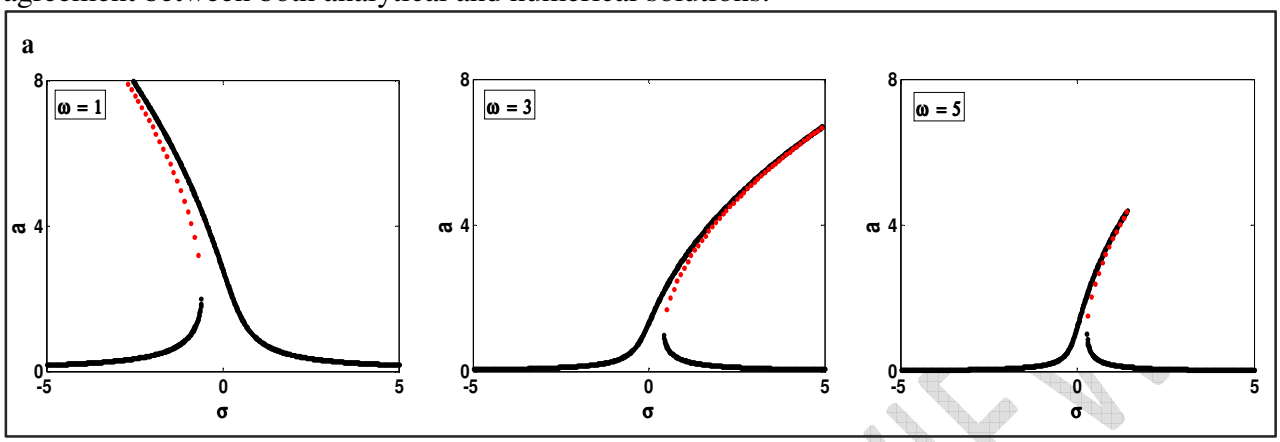

Fig. (7a): effect of ω, the values of the parameters are:
$\mu = 0.003, a_q = 1, a_c = 1, f = 1.8, G = 0.1, \tau = 0.1$.

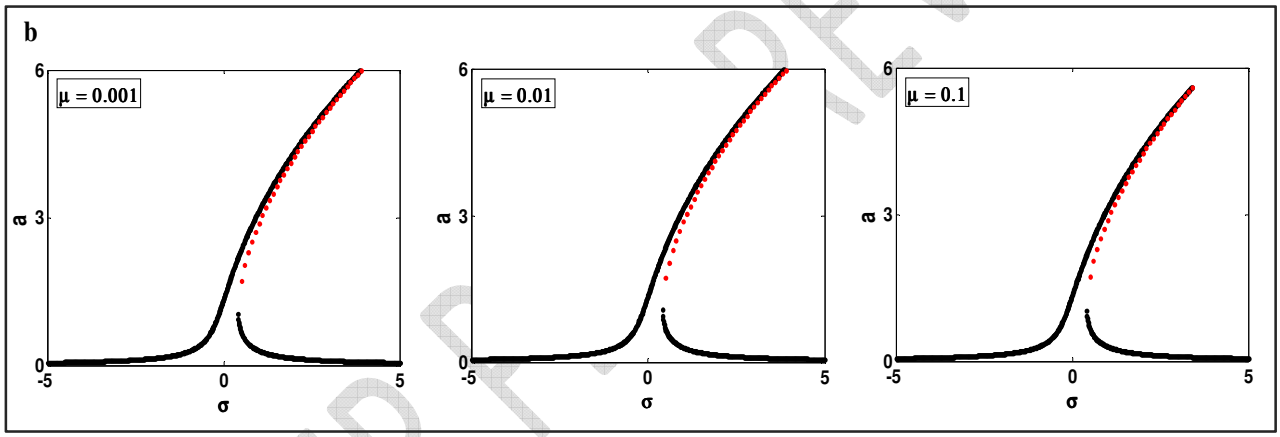

Fig. (7b): effect of μ, the values of the parameters are:
$\omega = 3.066, a_q = 1, a_c = 1, f = 1.8, G = 0.1, \tau = 0.1$.

UNDER PEER REVIEW

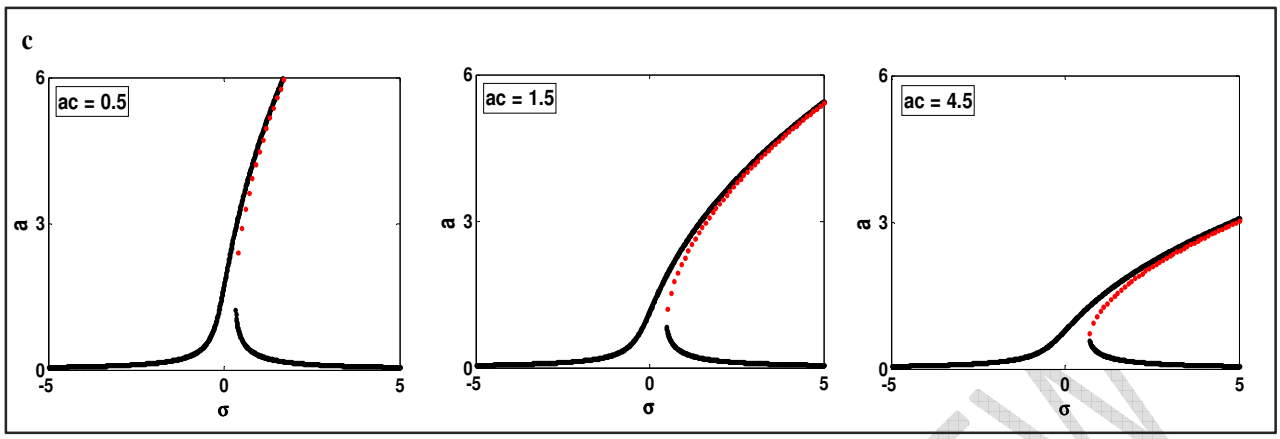

Fig. (7c): effect of a_c , the values of the parameters are:

$\omega = 3.066, \mu = 0.003, a_q = 1, f = 1.8, G = 0.1, \tau = 0.1$.

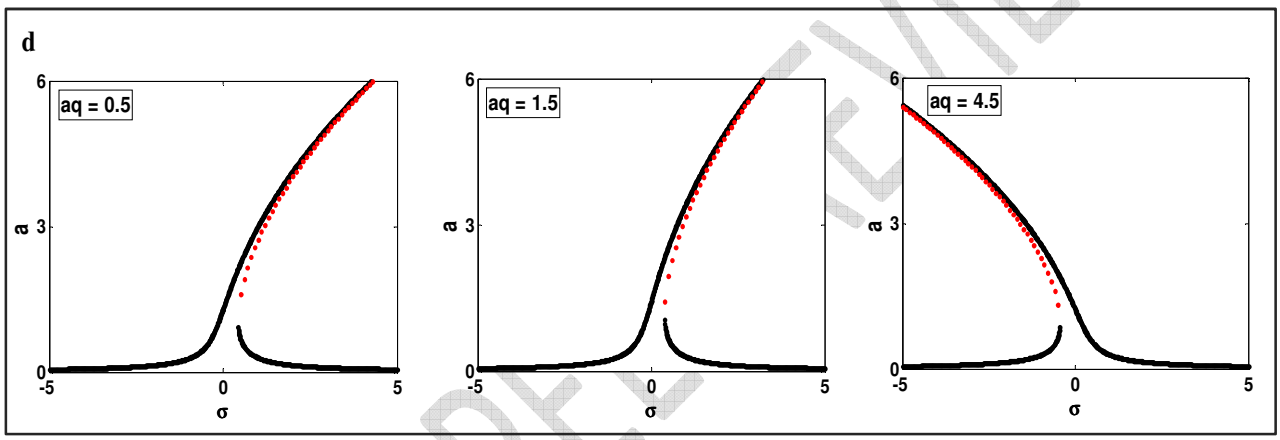

Fig. (7d): effect of a_q , the values of the parameters are:

$\omega = 3.066, \mu = 0.003, a_c = 1, f = 1.8, G = 0.1, \tau = 0.1$.

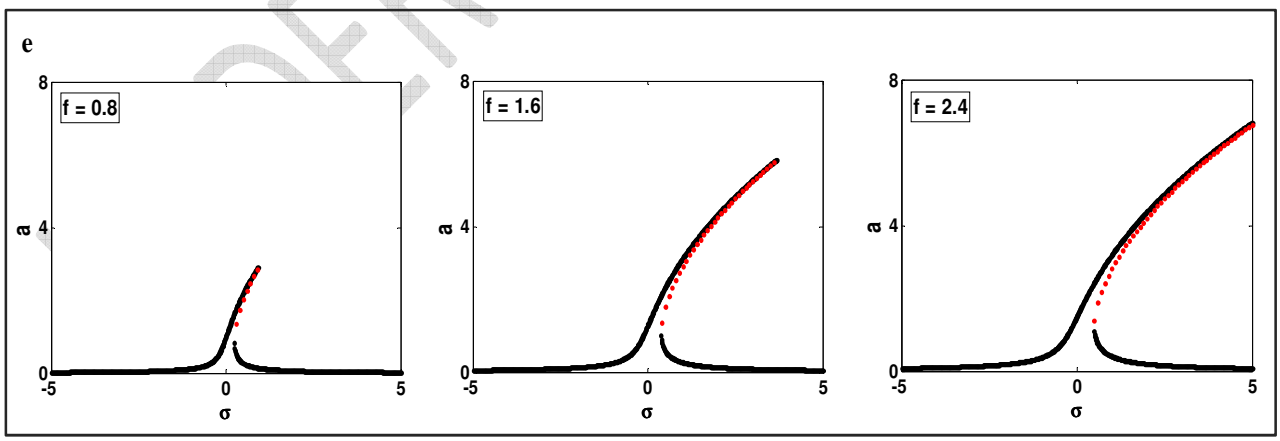

Fig. (7e): effect of f , the values of the parameters are:

$\omega = 3.066, \mu = 0.003, a_c = 1, a_q = 1, G = 0.1, \tau = 0.1$.

UNDER PEER REVIEW

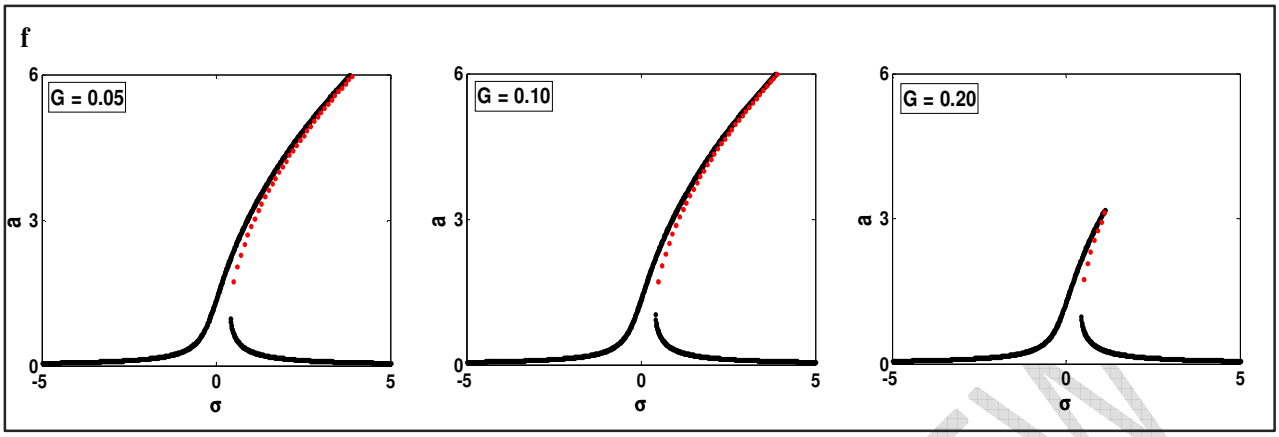

Fig. (7f): effect of G , the values of the parameters are:
$\omega = 3.066, \mu = 0.003, a_c = 1, a_q = 1, f = 1.8, \tau = 0.1$.

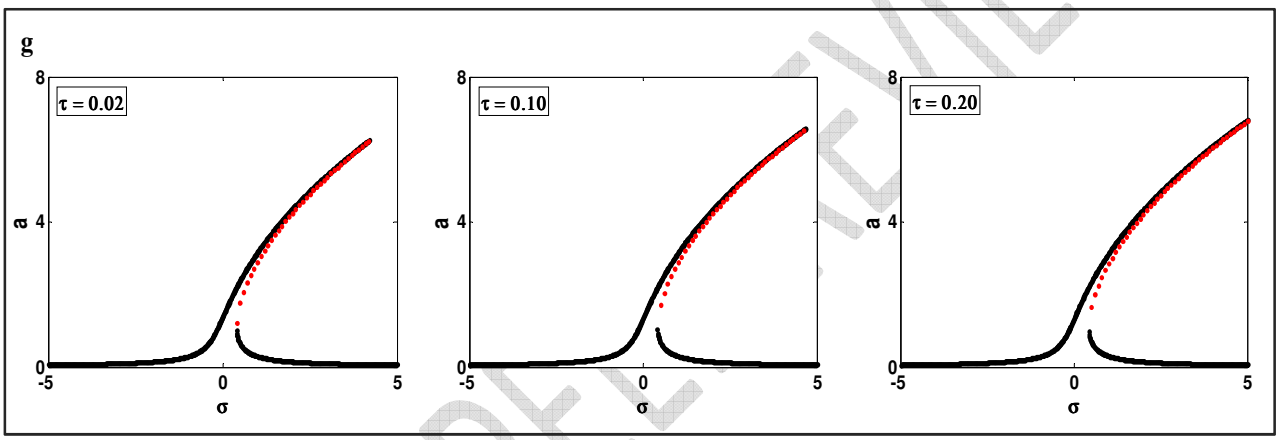

Fig. (7g): effect of τ , the values of the parameters are:
$\omega = 3.066, \mu = 0.003, a_c = 1, a_q = 1, f = 1.8, G = 0.1$.

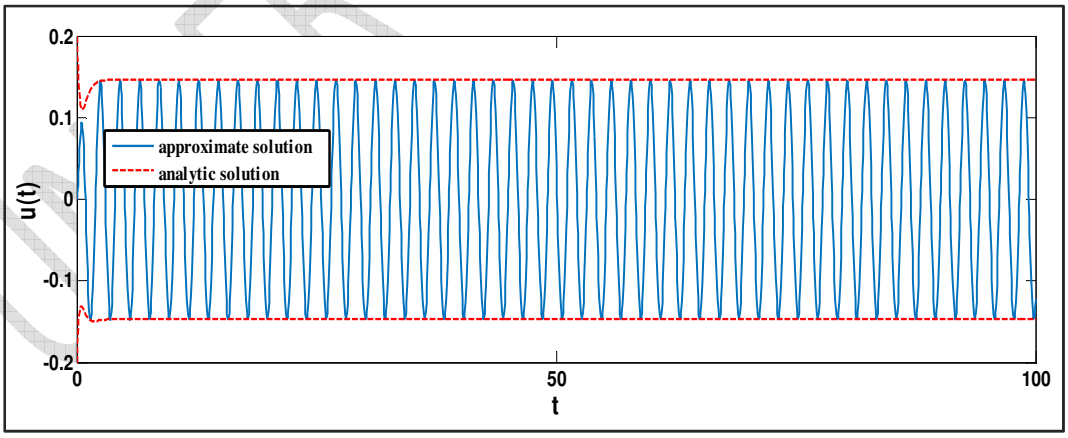

Fig. (8): Comparison between the analytic solution and the approximate solution at the case of time delay (Time history).

UNDER PEER REVIEW

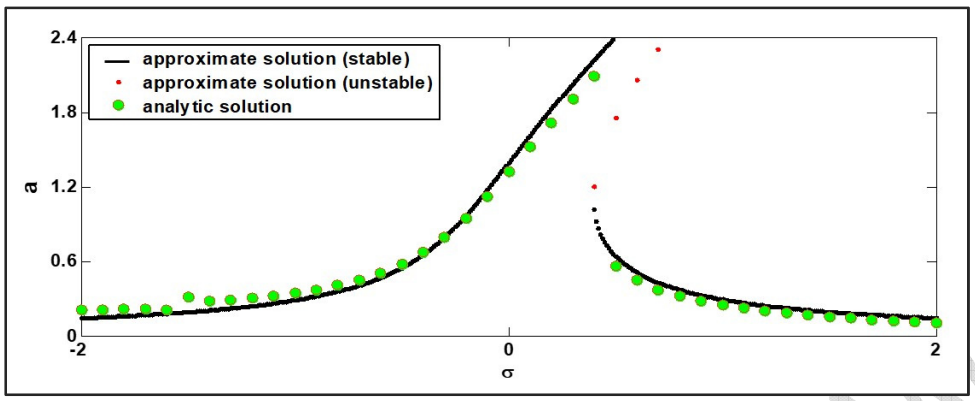

Fig. (9): Comparison between the analytic solution and the approximate solution at the case of time delay (Response curve).

4. Conclusion

The resulted vibration of a nonlinear dynamic mechanical system of electrostatic MEMS resonator subjected to external force has been studied to be controlled. Active control method is applied to reduce this vibration via negative linear velocity feedback. Also, time delay controller is used in reduction of the system vibration. The system is described by a unique differential equation. Multiple Scale Perturbation Technique (MSPT) is applied to determine an approximate solution for this system. The stability of the system near the primary resonance case is studied by applying the frequency response equation. A numerical integration of the system behavior without and with two controllers is studied. The results of this paper are reported:

1) Using negative gain feedback controller or time delay controller is effective in reduction about 93% of the system vibration amplitude.
2) The effect of the negative gain feedback controller and the time delay controller is similar in reduction of the system vibration amplitude.
3) The effectiveness of the controllers is about $E_a(u) = 2000$.

References

[1] B.Vazquez-Gonzalez and G.Silva-Navarro, Evaluation of the autoparametric pendulum vibration absorber for a Duffing system, Shock and Vibration, 15 (2008) 355-368.

[2] M. Eissa, M. Kamel and A. T. El-Sayed, Vibration reduction of a nonlinear spring pendulum under multi external and parametric excitations via a longitudinal absorber, Meccanica, 46 (2011) 325-340.

[3] M. Sayed and M. Kamel, 1:2 and 1:3 internal resonance active absorber for non-linear vibrating system, Applied Mathematical Modelling, 36 (2012) 310-332.

[4] D. Sado, The dynamics of a coupled three degree of freedom mechanical system, Mechanics and Mechanical Engineering, 7 (2004) 29-40.

[5] G. Wenzhi and H. Zhiyong, Active control and simulation test study on torsional vibration of large turbo-generator rotor shaft, Mechanism and Machine Theory, 45 (2010) 1326–1336.

[6] Y. A. Amer, H. S. Bauomy and M. Sayed, Vibration suppression in a twin-tail system to parametric and external excitation. Comput. Math. Appl., 58 (2009) 1947-1964.

[7] U. H. Hegazy and N. A. Salem, Nonlinear saturation controller for suppressing inclined beam vibrations, International Journal of Scientific & Engineering Research, 7 (2016) 964-974.

UNDER PEER REVIEW

[8] H. A. El-Gohary, W. A. A. El-Ganaini, Vibration suppression of a dynamical system to multi-parametric excitations via time delay absorber, Applied Mathematical Modelling, 36 (2012) 35-45.
[9] A. Maccari, Arbitrary amplitude periodic solutions for parametrically excited systems with time delay, Nonlinear Dynamics, 51 (2008) 111-126.
[10] A. M. Elnaggar and K. M. Khalil, The response of nonlinear controlled system under an external excitation via time delay state feedback, Journal of King Saud University – Engineering Sciences, 28 (2016) 75-83.
[11] A. F. El-Bassiouny and S. El-Kholy, Resonances of a nonlinear single-degree of freedom system with time delay in linear feedback control, Z. Naturforsch. 65a (2010) 357-368.
[12] Y. S. Hamed and Y. A. Amer, Nonlinear saturation controller for vibration suppression of a nonlinear flexible composite beam, J. Mech. Sci. Technol., 2 (2014) 2987-3002.
[13] M. Kamel, A. Kandil, W. A. El-Ganaini and M. Eissa, Active vibration control of a nonlinear magnetic levitation system via Nonlinear Saturation Controller (NSC), Nonlinear Dynamics, 77 (2014) 605-619.
[14] J. Warminski, M. P. Cartmell, A. Mitura and M. Bochenski, Active vibration control of a nonlinear beam with self and external excitations, Shock and Vibration, 20 (2013) 1033-1047.
[15] Y. A. Amer, Vibration control of ultrasonic cutting via dynamic absorber, Chaos, Solutions & Fractals, 33 (2007) 1703-1710.
[16] S. Ebrahimi, E. Salahshoor and M. Maasoomi, Application of the method of multiple scales for nonlinear vibration analysis of mechanical systems with dry and lubricated clearance joints, Journal of Theoretical and Applied Vibration and Acoustics, 3 (2017) 41-60.
[17] Y. A. Amer and M. N. Abd Elsalam, Stability and control of dynamical system subjected to multi external forces, International Journal of Mathematics and Computer, 3 (2013) 41-52.
[18] S. Shahlaei-Far, A. Nabarrete, J. M. Balthazar, Homotopy analysis of a forced nonlinear beam model with quadratic and cubic nonlinearities, Journal of Theoretical and Applied Mechanics, 54 (2016) 1219-1230.
[19] D. Wang, Z. Hao, Y. Chen and Y. Zhang, Dynamic and resonance response analysis for a turbine blade with varying rotating speed, Journal of Theoretical and Applied Mechanics, 56 (2018) 31-42.
[20] Y. S. Hamed, A. T. EL-Sayed and E. R. El-Zahar, On controlling the vibrations and energy transfer in MEMS gyroscope system with simultaneous resonance, Nonlinear Dynamics, 83 (2016) 1687-1704.
[21] A. Staino and B. Basu, Dynamics and control of vibrations in wind turbines with variable rotor speed, Engineering Structures, 56 (2013) 58-67.
[22] S. Shao, K.M. Masri and M.I. Younis, The effect of time-delayed feedback controller on an electrically actuated resonator, Nonlinear Dynamics, 74 (2013) 257-270.
[23] M. Daqaq, C. Reddy and A. Nayfeh, Input-shaping control of nonlinear MEMS, Nonlinear Dynamics, 54 (2008) 167-179.
[24] J. Feng, C. Liu, W. Zhang and S. Hao, Static and dynamic mechanical behaviors of electrostatic MEMS resonator with surface processing error, Micromachines, 9 (2018) 34.

UNDER PEER REVIEW